**Macromolecules**
ARTICLE

*Macromolecules* **2010**, *43*, 7931–7935 **7931**
DOI: 10.1021/ma101601e

# Direct Access to Polyisocyanide Screw Sense Using Vibrational Circular Dichroism

**Erik Schwartz,[†,§] Sérgio R. Domingos,[‡] Alexander Vdovin,[‡] Matthieu Koepf,[†,⊥] Wybren Jan Buma,[‡] Jeroen J. L. M. Cornelissen,*[,†,∥] Alan E. Rowan,*[,†] Roeland J. M. Nolte,*[,†] and Sander Woutersen*[,‡]**

[†]*Radboud University Nijmegen, Institute for Molecules and Materials, Heyendaalseweg 135, 6525 AJ Nijmegen, The Netherlands, and* [‡]*Van 't Hoff Institute for Molecular Sciences, University of Amsterdam, Nieuwe Achtergracht 166, 1018 WV Amsterdam, The Netherlands.* [§]*Present address: Department of Chemistry, The Scripps Research Institute, 10550 North Torrey Pines Road, La Jolla, California.* [∥]*Present address: Laboratory for Biomolecular Nanotechnology, MESA+ Institute, University of Twente, Enschede, The Netherlands.* [⊥]*Present address: Department of Chemistry & Biochemistry, Arizona State University, Tempe, Arizona.*

*Received July 16, 2010; Revised Manuscript Received August 17, 2010*

ABSTRACT: We show that the screw sense of polyisocyanide helices can be determined in a simple manner from the vibrational circular dichroism (VCD) of their CN-stretching mode. The relation between VCD and molecular structure is obtained using the coupled-oscillator approximation. It is shown that since the C═N groups point approximately radially outward from the helical axis, the CN-stretch region of the VCD spectrum of a polyisocyanide helix consists of a single couplet, the sign of which is directly related to the screw sense of the helix. We use this method to determine the screw sense of poly(*R*)-2-isocyanooctane and poly(*S*)-2-isocyanooctane from their VCD spectrum.

## Introduction

Inspired by the extraordinary functional properties of naturally occurring helical polymers like DNA and the α-helix, over the last decades an increasing number of scientists have designed and synthesized polymeric helical structures. After the pioneering work of Natta,[1] who found that highly isotactic polypropylene possesses a helical conformation in the crystalline state, chemists have been able to address the challenge to develop stable polymers with a preferred handedness to study their unique properties and their potential in the fields of material and supramolecular sciences. Just as in the case of naturally occurring helical polymers, the chemical and physical properties of synthetic helical polymers are strongly correlated with the conformation of their macromolecular backbone chains. A preferred polymer handedness can be achieved by the polymerization of the monomer using either chiral monomers or a chiral catalyst. Helical polymers,[2] such as sterically restricted polymethacrylate esters,[3] polychlorals,[4] polyguanidines,[5,6] or polyisocyanides,[7−9] with a high helix inversion barrier are considered to be stable when their helix inversion barrier exceeds ~85 kJ/mol.

Polyisocyanides, which were the first synthetic polymers to be reported to possess a stable helical conformation,[9] are prepared by the nickel(II) induced polymerization of isocyanide monomer units.[9−11] Restricted rotation around the single C−C bonds connecting the main-chain carbon atoms of the polymer gives rise to the formation of a stable helix, provided that the isocyanide-substituents are sufficiently bulky. Millich[7] proposed a $4_1$ helix (i.e., 4 repeat units per helical turn) for the main carbon chain in polyisocyanides. The helical conformation of polyisocyanides was confirmed by Nolte and co-workers[8] who resolved poly(*tert*-butyl isocyanide) into (+) and (−)-rotating fractions by using poly((*S*)-*sec*-butyl isocyanide) as a stationary phase during chromatographic purification. The helical conformation of polyisocyanides has been the subject of intensive debates in the last decades.[10,12−17] Despite the fact that various polyisocyanides have been synthesized,[11,18−21] it is not straightforward to determine their exact helical structures, in particular the helical pitch and helical sense.

Vibrational circular dichroism (VCD),[22] which has emerged as a powerful method to investigate the conformation of chiral molecules, seems an ideal probe to investigate the helical conformation of polyisocyanides. It has been demonstrated that the screw sense of helical polymers can often be determined from their VCD spectra. In general this is done by theoretically predicting (using quantum-chemical calculations) the VCD spectra of specific conformations of a molecule and comparing them with the experimentally observed one. This approach has been used successfully to investigate the structure of both biological[23−32] and synthetic[17,33−37] helical polymers.

On the other hand, the more simple, semiquantitative coupled-oscillator method, in which the molecular vibrations are treated as localized, interacting transition dipoles, still remains attractive because of its transparency and computational ease.[27,28,32,38−42] Here, we use this coupled-oscillator approach to interpret the VCD spectrum of the CN-stretching mode of polyisocyanides. It is shown that in the coupled-oscillator approximation, the coupled CN-stretching modes in a polyisocyanide helix give rise to a single VCD couplet and that the sign of the couplet provides a direct probe of the helical screw sense. We apply this method by determining the screw sense of two enantiomeric polyisocyanides from their VCD spectrum.

## Materials and Methods

The synthesis and characterization of the polyisocyanides used in this study are described in the Supporting Information. Fourier transform infrared (FTIR) and VCD spectra (with spectral resolutions of 2 and 4 cm$^{-1}$, respectively) were recorded on a Bruker Vertex 70 FTIR spectrometer in combination with a

---

*To whom correspondence should be addressed. E-mail: j.j.l.m.cornelissen@tnw.utwente.nl (J.J.L.M.C.); a.rowan@science.ru.nl (A.E.R.); r.nolte@science.ru.nl (R.J.M.N.); s.woutersen@uva.nl (S.W.).

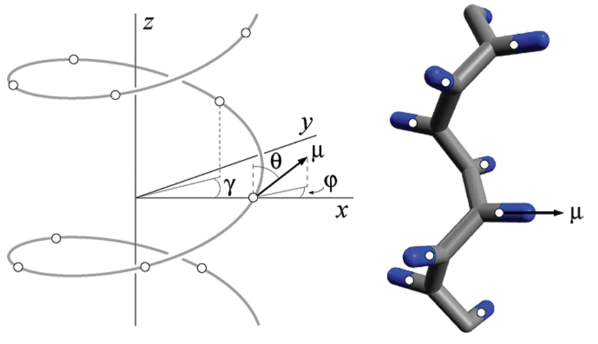

**Figure 1.** (Left) Schematic representation of a helical chain of transition-dipole moments, as specified by eq 1. The angles $\theta$ and $\phi$ that define the direction of the transition dipole moments $\mu$ with respect to the helical axis and the radius, respectively, have been indicated for the unit with $j = 0$. The CN bonds are at an angle $\theta$ with the helical axis. The projection of the CN bond on a plane perpendicular to the helical axis is at an angle $\phi$ with the radius (for the unit with $j = 0$ the radius coincides with the $x$ axis). (Right) Polyisocyanide backbone with $\phi = 0°$, $\theta = 90°$. The C═N transition dipoles are marked by white dots.

PMA 50 module. All spectra were recorded on 0.15 M solutions of the polyisocyanides in heptane. Samples were kept in sealed infrared sample cells consisting of 3 mm thick $CaF_2$ windows separated by a 0.5 mm spacer.

## Results and Discussion

**Relation between Helical Screw Sense and VCD.** Since the polyisocyanide polymers have a high persistence length,[43−45] we model them as infinitely long helices. To describe the vibrational absorption and the vibrational circular dichroism of an infinite helical array of C═N groups in the coupled-oscillator approximation, one can use the theory for the absorption and circular dichroism of helical aggregates of coupled, identical chromophores.[46−54] In the following, we use the notation of ref 51. Taking the helix to be aligned along the $z$-axis (see Figure 1) and numbering the units in the polymer by an integer $j$ (which runs from $-\infty$ to $\infty$ for an infinite polymer), the positions and directions of the transition-dipole moments can be written as

$$\begin{pmatrix} x_j \\ y_j \\ z_j \end{pmatrix} = \begin{pmatrix} r_0 \cos j\gamma \\ r_0 \sin j\gamma \\ hj \end{pmatrix} \quad \text{and} \quad \begin{pmatrix} \mu_j^x \\ \mu_j^y \\ \mu_j^z \end{pmatrix} = \mu \begin{pmatrix} \sin\theta\cos(j\gamma+\phi) \\ \sin\theta\sin(j\gamma+\phi) \\ \cos\theta \end{pmatrix} \tag{1}$$

respectively, with $r_0$ the radius of the helix, $\gamma$ the angle (relative to the helical axis) which separates consecutive units, $h$ their vertical separation, $\theta$ the angle of the transition-dipole moment with the helical axis, and $\phi$ the angle that the projection of $\vec{\mu}_j$ on the $xy$ plane makes with the radius. The above expressions are for a right-handed helix if $\gamma > 0$ and for a left-handed helix if $\gamma < 0$.

Since there is interaction between the transition dipoles, the energy eigenstates of the coupled-oscillator system are delocalized vibrational excitons. It can be shown from symmetry considerations[55] that only two eigenstates are IR active: the completely symmetric $A$ state and the doubly degenerate $E$ state. The frequencies of these two states are determined by the interactions between the chromophores in the helix:[51]

$$\omega_A = \omega_0 + {\sum_n}' J_n \tag{2}$$

$$\omega_E = \omega_0 + {\sum_n}' J_n \cos(n\gamma) \tag{3}$$

where $\omega_0$ is the frequency of an isolated C═N group, $J_n$ the interaction energy between the zeroth and $n$th C═N group, and the prime indicates that $n = 0$ is to be excluded from the summation. The absorption spectrum is given by[51]

$$A(\omega) = \frac{1}{3} N\mu^2[\cos^2\theta F_A(\omega - E_A) + \sin^2\theta F_E(\omega - E_E)] \tag{4}$$

where $N$ is the total number of chromophores, $\mu$ the transition-dipole moment of the $v = 0 \rightarrow 1$ transition of an isolated chromophore, and $F_{A,E}(\omega)$ the normalized line shape functions of the $A$ and $E$ bands.

It can be shown that the circular dichroism of the helix, defined as $R(\omega) = A_L(\omega) - A_R(\omega)$, is given by[50,51,54]

$$R(\omega) = \frac{N\mu^2\pi}{3}\left\{\frac{r_0}{2\lambda}\sin 2\theta \sin\phi[F_A(\omega-\omega_A) - F_E(\omega-\omega_E)] + \frac{h}{2\lambda}\sin^2\theta F_E'(\omega-\omega_E){\sum_n}' n\sin(n\gamma)J_n\right\} \tag{5}$$

where $F_E'(\omega)$ is the first derivative of the $E$ line shape with respect to $\omega$, $\lambda$ the optical wavelength, and $J_n$ the interaction energy between the $m$th and $(m+n)$th transition dipole moment (which is independent of $m$ because of the helical symmetry). The two terms in this equation each represent a VCD couplet but with different physical origins. The first term is a VCD couplet due to the frequency splitting between the $A$ and $E$ modes. This term is nonzero if $\phi$ is nonzero and $\theta$ is neither 0° nor 90°. In that case, both the $A$ and $E$ modes exhibit VCD, with equal magnitudes but opposite signs, giving rise to a VCD couplet.[46,47] The second VCD term in eq 5 arises from the absorption of circularly polarized light traveling along the helical axis.

**Simplifications for Polyisocyanides.** Polyisocyanides represent a class of helices for which the above equations simplify significantly. In polyisocyanides, the projection of the C═N bond on the $xy$ plane is to a good approximation perpendicular to the helical axis, so we have $\phi = 0°$ (see Figure 1). Consequently, the first term in eq 5 vanishes so that the VCD spectrum consists purely of the helical VCD couplet, which is the derivative of the $E$ absorption band. To establish the relation between the screw sense and the sign of this VCD couplet, we use the fact that nearest-neighbor interaction dominates, so that the summation in eq 5 reduces to $2J_1 \sin\gamma$, where $J_1$ is the nearest-neighbor interaction energy. We then have

$$R(\omega) = \frac{N\mu^2\pi h}{3\lambda}\sin^2\theta F_E{}'(\omega-\omega_E)J_1\sin\gamma \tag{6}$$

Since in polyisocyanides the nearest-neighbor C═N transition dipoles have charges with the same sign approaching each other, we have $J_1 > 0$ (this is confirmed by a density-functional calculation, see Supporting Information). Hence, the VCD spectrum of a right-handed polyisocyanide ($\gamma = +90°$, so $\sin\gamma = 1$ in eq 6) is proportional to the derivative of the $E$ absorption band, whereas the VCD spectrum of a left-handed polyisocyanide ($\gamma = -90°$) is proportional to the derivative of the $E$ absorption band multiplied by $-1$. We thus have a simple and direct relation between the screw sense of a polyisocyanide and its CN-stretch VCD spectrum: for a right-handed polyisocyanide the CN-stretch VCD spectrum is the derivative of the CN-stretch band (positive signal on the lower frequency side, and negative on the higher frequency side of the absorption band), whereas for a left-handed helix it is the negative derivative of the absorption band (negative on the lower frequency side and positive on the higher frequency side of the absorption band).

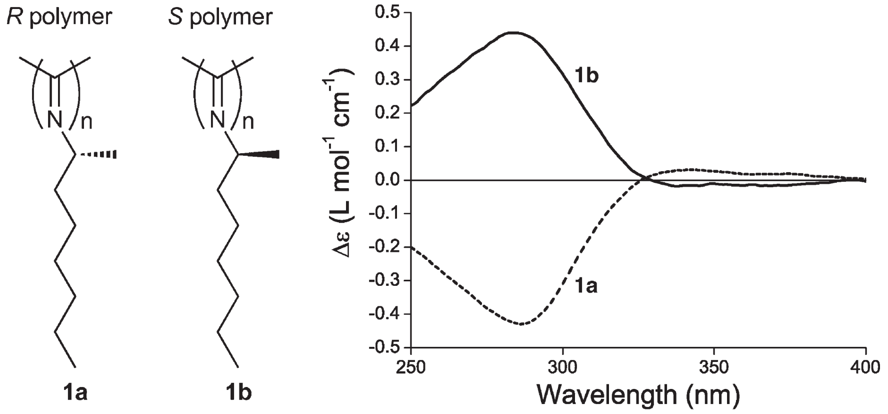

**Figure 2.** Chemical structures (left) and CD spectra (right) of the two enantiomeric polyisocyanides studied here.

An even stronger simplification occurs if the C═N bonds are perpendicular to the helical axis (that is, they are in the *xy* plane), so that $\theta = 90°$. This reduces the first term in eq 4 to zero, so that the absorption spectrum consists of the *E* band only,

$$A(\omega) = \frac{1}{3} N\mu^2 F_E(\omega - \omega_E) \tag{7}$$

In the case that the C═N bonds are not exactly perpendicular to the helical axis, there will be a weak *A*-band present in the absorption spectrum.

Interestingly, from the ratio of $R(\omega)$ (the VCD spectrum) and $A_E'(\omega)$ (the derivative of the *E* absorption band with respect to $\omega$), we can obtain an independent estimate for the nearest-neighbor interaction $J_1$. Combining eqs 6 and 7, we find that

$$\frac{R(\omega)}{A_E'(\omega)} = \frac{\pi h J_1}{\lambda} \tag{8}$$

where $A_E'(\omega)$ is the derivative of the *E* absorption band with respect to $\omega$. This shows that the ratio of the VCD and the derivative of the absorption spectrum is determined by the nearest-neighbor interaction $J_1$ and a single geometrical parameter of the helix, the vertical separation *h* between two consecutive units.

**Application to Poly(2-isocyanooctane).** We use the relation between the CN-stretch VCD of polyisocyanides and their screw sense to determine the screw sense of the enantiomeric helical polyisocyanides poly(*R*)-2-isocyanooctane **1a** and poly(*S*)-2-isocyanooctane **1b**, see Figure 2. We first determined the screw sense of these polymers independently using UV circular dichroism (CD). Although optical rotation values can be used to obtain information about the conformations of the polymer, in this case the rigid environment of the polymer $(\mathrm{RN{=}C})_n$ might affect the conformation of the R substituent and thus its contribution to the optical rotation. In the CD spectrum, the $n-\pi^*$ transition of the backbone imine functions can be monitored. The CD spectrum of **1** in heptane in the region $\lambda = 250-400$ nm, depicted in Figure 2, corresponds to this transition. In the polymer, both the chiral center in the side chain as well as the helical structure of the main chain will induce rotational power in the C═N group.[56] The large negative band of **1a** (positive band for **1b**) with a maximum $\Delta\varepsilon$ at $\lambda = 285$ nm is attributed to the influence of the chiral side chain on the $n-\pi^*$ transitions. In theory, the helicity (screw sense) of the polymer can be derived from the sign sequence of the exciton couplet by a comparison with a model compound, for example, poly(*tert*-butyliminomethylene), from which the screw sense was obtained by a resolution process.[57] In Figure 2, this couplet is not clearly visible because of the overlap with the contribution that arises from the influence of the chiral side chain on the $n-\pi^*$ transition, but the asymmetry of the curve is a first indication. On careful inspection of the curves, a positive band at $\lambda = 320$ nm, as part of the positive couplet evident for the helicity, can be observed.[58] Such a couplet was also observed for (*M*)-poly(*tert*-butyliminomethylene), and thus, by looking at the similarity of the couplets, it can be tentatively conclude that polymer **1a** is predominantly in the *M*-helical conformation. In this way, however, the screw sense is determined by an indirect method and the assignment of the exciton couplet is hampered by side chain contributions to the Cotton effect originating from the backbone $n-\pi^*$ transitions.

In contrast, the CN-stretch VCD spectrum provides direct access to the polyisocyanide screw sense. The vibrational absorption spectrum of these polyisocyanides, shown in Figure 3, contains a CN-stretch band with a shoulder on the high-frequency side. We find that the isocyanide monomer exhibits negligible VCD (see Supporting Information), so that the VCD of the polymer arises from interaction between the CN-stretch dipoles. The strong peak and the shoulder in the spectrum can be assigned to the two optically allowed modes using eq 4. Since the projection of the transition dipoles on the helical axis is small ($\theta \approx 90°$), the absorption intensity of the *A* mode will be small compared to that of the *E* modes. We therefore assign the main peak to the *E* mode and the weaker high-frequency shoulder to the *A* mode. By least-squares fitting two Lorentzian line shapes to the spectrum, we obtain center frequencies for the *E* and *A* transitions of 1635 and 1643 $\mathrm{cm}^{-1}$, respectively. Assuming that the nearest-neighbor interaction $J_1$ between CN-groups dominates (see above), one expects from eqs 2 and 3 a frequency difference $\omega_A - \omega_E = 2J_1$. Our assignment of the bands consequently implies a nearest-neighbor interaction $J_1$ of $+\,4\ \mathrm{cm}^{-1}$. This experimental value for the coupling may be compared to a theoretical prediction using the dipole−dipole approximation. In this approximation, which has been found to give a fairly accurate quantitative description of several different molecular systems,[59−63] the coupling between two C═N-stretch modes *a* and *b* is given by[59]

$$J_{ab} = \frac{1}{4\pi\varepsilon_0}\left[\frac{\vec{\mu}_a\cdot\vec{\mu}_b}{r_{ab}^{3}} - 3\,\frac{(\vec{r}_{ab}\cdot\vec{\mu}_a)(\vec{r}_{ab}\cdot\vec{\mu}_b)}{r_{ab}^{5}}\right] \tag{9}$$

where $\vec{\mu}_{a,b}$ are the CN-stretch transition dipoles and $\vec{r}_{ab}$ is the distance vector between the two transition dipoles. The

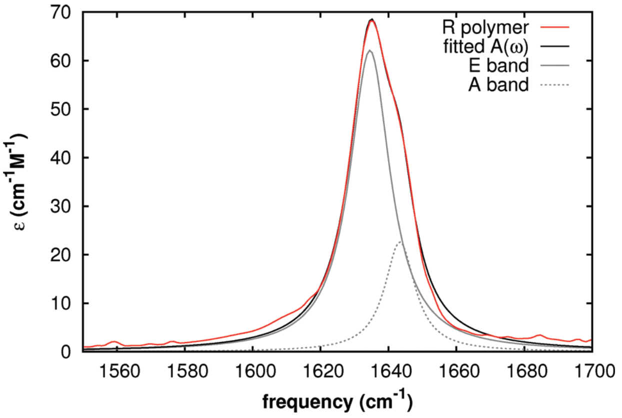

**Figure 3.** Infrared absorption spectrum of **1a**, together with a least-squares fit of two Lorentzian lineshapes. The spectrum of the *S*-polymer is identical to that of the *R*-polymer.

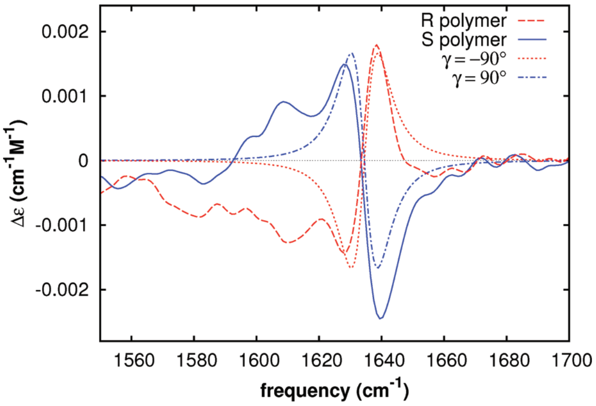

**Figure 4.** Vibrational circular dichroism spectra of the *R*- and *S*-polymers, together with eq 6 for $\gamma = +90°$ (right-handed helix) and $\gamma = -90°$ (left-handed helix).

magnitude of the CN-stretch transition-dipole moment can be determined from the integrated absorption coefficient,[64] and from the experimental FTIR spectrum (Figure 3), we obtain $|\vec{\mu}| = 0.089$ D. Using the geometrical parameters of the polyisocyanide helix ($r = 2.3$ Å, $\angle(\vec{\mu}_i, \vec{\mu}_{i+1}) = 90°$, $\angle(\vec{\mu}_i, \vec{r}_{i,i+1}) = 56°$),[43] we find $J_1 = 7$ cm$^{-1}$. This implies an $\omega_A - \omega_E$ frequency splitting of 14 cm$^{-1}$, which agrees reasonably well (both in sign and magnitude) with the experimental value of 8 cm$^{-1}$, thus confirming our assigment of the strong absorption band to the *E* mode and of the shoulder to the *A* mode. The discrepancy between the experimental and calculated freqeuncy splittings is probably due to the breakdown of the dipolar approximation at short dipole−dipole distance, leading to an overestimation of the coupling. Further confirmation of the assignment of the shoulder to the *A* mode was obtained from a density-functional calculation on a 16-mer helical polyisocyanide (see the Supporting Information for details). From this calculation we obtain an $\omega_A - \omega_E$ splitting of 11.5 cm$^{-1}$, which agrees even better with the experimentally observed value.

The VCD spectra in the CN-stretching region of the two enantiomeric polymers are shown in Figure 4. These spectra indeed contain a couplet centered at the frequency of the *E* absorption band, as predicted by the theoretical analysis. They also contain a singlet feature at lower frequency (around 1610 cm$^{-1}$), which we cannot at present assign, since no corresponding absorption band is present in the absorption spectrum (Figure 3). As shown in Figure 4 (dashed−dotted and dotted curves), we find that in the CN-stretch region, the VCD spectra of the *R*-polymer can be well described by the negative derivative of the *E* absorption band, whereas the VCD of the *S*-polymer corresponds to the VCD spectrum predicted for a right-handed helix.

As a cross check for interpretation of the VCD spectrum, we now use eq 8 to obtain an independent estimate for the nearest neighbor interaction $J_1$, which was estimated to be 4 cm$^{-1}$ from the splitting between the two CN-stretch peaks observed in the absorption spectrum. Substituting the known[43] vertical separation $h = 0.10$ nm and the wavelength of the light $\lambda = 6.1$ $\mu$m, we obtain from the experimental ratio $R(\omega)/A_E'(\omega)$ of $\approx 0.0019$ an estimate of $J_1 \approx 6$ cm$^{-1}$ (note that the value for $J_1$ obtained from eq 8 is expressed in angular frequency units and must be divided by $2\pi$ to obtain the value in normal frequency units). This estimate for $J_1$ agrees reasonably well with the value of 4 cm$^{-1}$ obtained from the splitting between the *E* and *A* CN-stretch bands (see above), which confirms the validity of our interpretation of the CN-stretch VCD couplet in terms of a coupled-oscillator model.

## Conclusions

We have shown that a polyisocyanide has a very simple CN-stretch VCD spectrum if it has a backbone geometry with $\phi \approx 0°$, i.e., if the CN bonds (or more generally, the projections of the CN bonds on the plane perpendicular to the helical axis) point approximately radially outward. In that case, the CN-stretch VCD spectrum consists of a single couplet, which is caused purely by helical VCD. The screw sense of a polyisocyanide helix can then be determined directly from the sign of this couplet, without any need for additional calculations.

There might be polyisocyanides for which a more detailed analysis than the one presented here is required to obtain the screw sense. In particular, bulky side groups might render $\phi$ very different from zero, and aryl side groups might influence the interaction between the CN-stretch modes in the backbone of the helix. In general, however, the details of the polyisocyanide side chains will not be important for the interpretation of the CN-stretch VCD spectrum. We therefore expect the simple relation between VCD and screw sense presented here to be usable for many polyisocyanides.

**Acknowledgment.** S. R. Domingos acknowledges financial support by the Portuguese FCT through Project No. SFRH/BD/48295/2008. The researchers at the Radboud University Nijmegen acknowledge the Technical Foundation STW for financial support.

**Supporting Information Available:** Description of the synthesis and characterization of the polymers studied, additional measurements on the isocyanide monomer, and the results of the DFT calculation on a 16-mer polyisocyanide. This material is available free of charge via the Internet at http://pubs.acs.org.

## References and Notes

(1) Natta, G.; Pino, P.; Corradini, P.; Danusso, F.; Mantica, E.; Mazzanti, G.; Moraglio, G. *J. Am. Chem. Soc.* **1955**, *77*, 1708–1710.
(2) Yashima, E.; Maeda, K.; Iida, H.; Furusho, Y.; Nagai, K. *Chem. Rev.* **2009**, *109*, 6102–6211.
(3) Okamoto, Y.; Yashima, E. *Prog. Polym. Sci.* **1990**, *15*, 263–298.
(4) Ute, K.; Hirose, K.; Kashimoto, H.; Hatada, K.; Vogl, O. *J. Am. Chem. Soc.* **1991**, *113*, 6305–6306.
(5) Tang, H.-Z.; Lu, Y. J.; Tian, G. L.; Capracotta, M. D.; Novak, B. M. *J. Am. Chem. Soc.* **2004**, *126*, 3722–3723.
(6) Tang, H.-Z.; Novak, B. M.; He, J. T.; Polavarapu, P. L. *Angew. Chem., Int. Ed.* **2005**, *44*, 7298–7301.

(7) Millich, F. *Chem. Rev.* **1972**, *72*, 101–113.
(8) Nolte, R. J. M.; van Beijnen, A. J. M.; Drenth, W. *J. Am. Chem. Soc.* **1974**, *96*, 5932–6933.
(9) Nolte, R. J. M. *Chem. Soc. Rev.* **1994**, *23*, 11–19.
(10) Suginome, M.; Ito, Y. *Adv. Polym. Sci.* **2004**, *171*, 77–136.
(11) Cornelissen, J. J. L. M.; Donners, J. J. J. M.; de Gelder, R.; Glaswinkel, W. S.; Metselaar, G. A.; Rowan, A. E.; Sommerdijk, N. A. J. M.; Nolte, R. J. M. *Science* **2001**, *293*, 676–680.
(12) Green, M. M.; Gross, R. A.; Schilling, F. C.; Zero, K.; Crosby, C., III *Macromolecules* **1988**, *21*, 1839–1846.
(13) Kollmar, C.; Hoffman, R. *J. Am. Chem. Soc.* **1990**, *112*, 8230–8328.
(14) Deming, T. J.; Novak, B. M. *J. Am. Chem. Soc.* **1993**, *115*, 9101–9111.
(15) Clericuzio, M.; Alagona, G.; Ghio, C.; Salvadori, P. *J. Am. Chem. Soc.* **1997**, *119*, 1059–1071.
(16) Takei, F.; Onitsuka, K.; Takahashi, S. *Macromolecules* **2005**, *38*, 1513–1516.
(17) Hase, Y.; Nagai, K.; Iida, H.; Maeda, K.; Ochi, N.; Sawabe, K.; Sakajiri, K.; Okoshi, K.; Yashima, E. *J. Am. Chem. Soc.* **2009**, *131*, 10719–10732.
(18) Takei, F.; Hayashi, H.; Kobayashi, K. O. N.; Takahashi, S. *Angew. Chem., Int. Ed.* **2001**, *40*, 4092–4094.
(19) Gomar-Nadal, E.; Veciana, J.; Rovira, C.; Amabilino, D. B. *Adv. Mater.* **2005**, *17*, 2095–2098.
(20) Kajitani, T.; Okoshi, K.; Sakurai, S.-I.; Kumaki, J.; Yashima, E. *J. Am. Chem. Soc.* **2006**, *128*, 708–709.
(21) Schwartz, E.; Bodis, P.; Koepf, M.; Cornelissen, J. J. L. M.; Rowan, A. E.; Woutersen, S.; Nolte, R. J. M. *Chem. Commun.* **2009**, 4675–4677.
(22) Nafie, L. A.; Keiderling, T. A.; Stephens, P. J. *J. Am. Chem. Soc.* **1976**, *98*, 2715–2723.
(23) Lal, B. B.; Nafie, L. A. *Biopolymers* **1982**, *21*, 2161–2183.
(24) Sen, A. C.; Keiderling, T. A. *Biopolymers* **1984**, *23*, 1519–1532.
(25) Lipp, E. D.; Nafie, L. A. *Biopolymers* **1985**, *24*, 799–812.
(26) Paterlini, M. G.; Freedman, T. B.; Nafie, L. A. *Biopolymers* **1986**, *25*, 1751–1765.
(27) Zhong, W.; Gulotta, M.; Goss, D. J.; Diem, M. *Biochemistry* **1990**, *29*, 7485–7491.
(28) Xiang, T.; Goss, D. J.; Diem, M. *Biophys. J.* **1993**, *65*, 1255–1261.
(29) Dukor, R. K.; Keiderling, T. A. *Biospectroscopy* **1996**, *2*, 83–100.
(30) Andrushchenko; Wieser, H.; Bouř, P. *J. Phys. Chem. B* **2004**, *108*, 3899–3911.
(31) Bouř, P.; Andrushchenko, V.; Kabeláč, M.; Maharaj, V.; Wieser, H. *J. Phys. Chem. B* **2005**, *109*, 20579–20587.
(32) Krummel, A. T.; Zanni, M. T. *J. Phys. Chem. B* **2006**, *110*, 13991–14000.
(33) Buffeteau, T.; Ducasse, L.; Poniman, L.; Delsuc, N.; Huc, I. *Chem. Commun.* **2007**, 2714–2716.
(34) Ducasse, L.; Castet, F.; Fritsch, A.; Huc, I.; Buffeteau, T. *J. Phys. Chem. A* **2007**, *111*, 5092–5098.
(35) Tang, H.-Z.; Garland, E. R.; Novak, B. M.; He, J.; Polavarapu, P. L.; Sun, F. C.; Sheiko, S. S. *Macromolecules* **2007**, *40*, 3575–3580.
(36) Smulders, M. M. J.; Buffeteau, T.; Cavagnat, D.; Wolffs, M.; Schenning, A. P. H. J.; Meijer, E. W. *Chirality* **2008**, *20*, 1016–1022.
(37) Kawauchi, T.; Kitaura, A.; Kumaki, J.; Kusanagi, H.; Yashima, E. *J. Am. Chem. Soc.* **2008**, *130*, 11889–11891.
(38) Keiderling, T. A.; Stephens, P. J. *J. Am. Chem. Soc.* **1977**, *99*, 8061–8062.
(39) Eker, F.; Cao, X. L.; Nafie, L.; Schweitzer-Stenner, R. *J. Am. Chem. Soc.* **2002**, *124*, 14330–14341.
(40) Eker, F.; Griebenow, K.; Cao, X. L.; Nafie, L.; Schweitzer-Stenner, R. *Proc. Natl. Acad. Sci. U.S.A.* **2004**, *101*, 10054–10059.
(41) Schweitzer-Stenner, R. *J. Phys. Chem. B* **2004**, *108*, 16965–16975.
(42) Choi, J.-H.; Hahn, S.; Cho, M. *Int. J. Quantum Chem.* **2005**, *104*, 616–634.
(43) Beijnen, A. J. M. V.; Nolte, R. J. M.; Drenth, W. *Tetrahedron* **1967**, *32*, 2017–2019.
(44) Okoshi, K.; Nagai, K.; Kajitani, T.; Sakurai, S.-i.; Yashima, E. *Macromolecules* **2008**, *41*, 7752–7754.
(45) Samori, P.; Ecker, C.; Gossl, I.; de Witte, P.; Cornelissen, J.; Metselaar, G.; Otten, M.; Rowan, A.; Nolte, R.; Rabe, J. *Macromolecules* **2002**, *35*, 5290–5294.
(46) Moffitt, W. *J. Chem. Phys.* **1956**, *25*, 467–478.
(47) Moffitt, W. *Proc. Natl. Acad. Sci. U.S.A.* **1957**, *43*, 723–730.
(48) Tinoco, I.; Woody, R. W. *J. Chem. Phys.* **1963**, *38*, 1317–1325.
(49) Woody, R. W.; Tinoco, I., Jr *J. Chem. Phys.* **1967**, *46*, 4927–4945.
(50) Somsen, O. J. G.; van Grondelle, R.; van Amerongen, H. *Biophys. J.* **1996**, *71*, 1934–1951.
(51) Didraga, C.; Klugkist, J. A.; Knoester, J. *J. Phys. Chem. B* **2002**, *106*, 11474–11486.
(52) Didraga, C.; Knoester, J. *J. Chem. Phys.* **2004**, *121*, 946–959.
(53) Woody, R. W. *Monatsh. Chem.* **2005**, *136*, 347–366.
(54) Eisfeld, A.; Kniprath, R.; Briggs, J. S. *J. Chem. Phys.* **2007**, *126*, 104904.
(55) Higgs, P. W. *Proc. R. Soc. London, Ser. A* **1953**, *133*, 472–485.
(56) Tinoco, I. *J. Chim. Phys. PCB* **1968**, *65*, 91–97.
(57) van Beijnen, A. J. M.; Nolte, R. J. M.; Drenth, W. *Tetrahedron* **1976**, *32*, 2017–2019.
(58) Schellman, J. A. *Acc. Chem. Res.* **1968**, *1*, 144–151.
(59) Krimm, S.; Bandekar, J. *Adv. Protein Chem.* **1986**, *38*, 181–364.
(60) Hamm, P.; Lim, M.; Hochstrasser, R. M. *J. Phys. Chem. B* **1998**, *102*, 6123–6138.
(61) Krummel, A. T.; Mukherjee, P.; Zanni, M. T. *J. Phys. Chem. B* **2003**, *107*, 9165–9169.
(62) Demirdoven, N.; Cheatum, C. M.; Chung, H. S.; Khalil, M.; Knoester, J.; Tokmakoff, A. *J. Am. Chem. Soc.* **2004**, *126*, 7981–7990.
(63) Dijkstra, A. G.; Knoester, J. *J. Phys. Chem. B* **2005**, *109*, 9787–9798.
(64) Sturm, J. E. *J. Chem. Educ.* **1990**, *67*, 32–33.